Chapter 3

Synthesis and Optical Properties of Highly Stabilized Peptide-Coated Silver Nanoparticles

Parvathalu Kalakonda and Sreenivas Banne

Additional information is available at the end of the chapter

http://dx.doi.org/10.5772/intechopen.76829

Abstract

The interaction between the silver nanoparticle and peptide surfaces has been of increased interest for the applications of bionanotechnology and tissue engineering. In order to completely understand such interactions, we have examined the optical properties of peptide-coated silver nanoparticles. However, the effect of peptide binding motif upon the silver nanoparticles surface characteristics and physicochemical properties of these nanoparticles remains incompletely understood. Here, we have fabricated sodium citrate stabilized silver nanoparticles and coated with peptide IVD (ID_3). The optical properties of these peptide-capped nanomaterials were characterized by UV-visible, transmission electron microscopy (TEM), and z-potential measurement. The results indicate that the interface of silver nanoparticles (AgNP)-peptide is generated using ID_3 peptide and suggested that the reactivity of peptide is governed by the conformation of the bound peptide on the silver nanoparticle surface. The interactions of peptide-nanoparticle would potentially be used to fabricate specific functionality into the various peptide-capped nanomaterials and antibacterial applications.

Keywords: silver nanoparticles, peptide, Z-potential, physicochemical properties

1. Introduction

Over the last few years, the fabrication and synthesis of stable silver nanoparticles are the most leading active areas of research in the field of bionanotechnology due to their wide range of applications in areas such as biosensing, biotechnology, biolabeling, biomedical, and antibacterial applications [1–8]. The properties of nanoparticles would be modified by capping certain functional groups to change their biocompatibility and stability in many biological

systems [9, 10]. The major challenge is maintaining the size control and distribution of these particles into the biological environment. The nanoparticles' size plays a very important role and it should be of a suitable size between 20 and 100 nm to avoid the negative charge and renal clearance [11]. The physical and chemical properties of nanoparticles can be changed rapidly by the adsorption of proteins which enable them to help cellular internalization [12]. In addition, opsonization can result in an undesired cellular uptake, nanoparticle aggregation, and an immune system response [13].

The available methods for creating "stealth" nanoparticles that resist nonspecific protein adsorption include surface modification by polyethylene glycol (PEG) [14], polysaccharides [15], mixed charge self-assembly [16], and polymers [17, 18]. An attractive way for stealth coatings is to study the use of natural materials such as peptides: they are biocompatible, biodegradable, well-studied, non-immunogenic, and multifunctional materials [19]. Over the last few years, antibacterial peptides have become huge interesting diagnosis tools for improving new techniques for the production of novel antibiotics in the treatment of human infections [20]. The antimicrobial activity of AgNP nanoparticles has been communicated extensively in the area of killing Gram-negative and Gram-positive bacteria [21, 22]. Silver nanoparticles are more toxic element to microorganism compared to other metals and they exhibit slow toxicity into cells. They have an advantage of lower propensity to induce microbial resistance [23, 24]. The protein-coated nanoparticles have been well studied to fabricate stable systems in buffered saline systems (PBS) [25, 26]. However, by improving the nanoparticles stability in complex fluids, we can use as undiluted human serum is very challenging than in buffered saline solution due to the presence of huge proteins. And also, the interactions between peptides and peptide-bound nanoparticles were not yet well studied. It is very important to investigate nanoparticles properties in complex fluids before performing in vivo experiments. Developing peptide-coated-AgNP materials that are stable in complex fluids increases in vivo applications. In addition to possessing stealth properties, it is very useful to incorporate specific interactions of peptide with nanoparticles for biomedical technology applications. The peptide sequences have a particular molecular recognition for receptors on various cell types. However, additional conjugation steps are important to change peptide targeting sequences onto stealth particles which contain synthetic polymers such as PEG [27, 28]. Peptide capping offers many advantages due to their sequence and can be applied off for the existing peptide sequence [29, 30]. Combining the s-peptide sequence with a targeting moiety leads to specific interactions with maintaining a low fouling background, and the complex fluids increase the stability of nanoparticles by peptide coating.

In this work, we have examined a synthetic peptide of IVD (ID3) [31]. The sequence mimics is important and the surfaces of proteins have adapted to avoid nonspecific adsorption. This leads to improve the stability of nanoparticles in complex fluids. Here, charge neutrality is balanced by leaving the N-terminus amine which is free ion, and it contributes to an extra positive charge to the peptide. The peptide sequence was attached to nanoparticles such as AgNP through a surface anchoring via covalent bonding. The zeta potential and optical spectroscopy (UV-visible) results indicate that peptide-anchored silver nanoparticles show high stability in complex fluids. The functional peptide always contains biomolecular recognition. Moreover, the advantages of this system are easily fabricated in a one-step process by mixing silver nanoparticles and self-assembling peptides.

http://dx.doi.org/10.5772/intechopen.76829

2. Experimental section

2.1. Materials and methods

Peptide (ID_3) with confirmed amino acid analysis was purchased from the American Peptide Company. Silver nitrate ($AgNO_3$) and citric acid tri-sodium salt dehydrate were purchased from Fisher Scientific (Waltham, MA). The peptide content varied between 70 and 85%, and the ID_3 peptide was acetylated at the N-terminus. All solvents were purchased from Sigma-Aldrich Co.

2.1.1. Synthesis

Silver nanoparticles were synthesized by reduction method. Hundred milligrams of silver nitrate was dissolved in 500 ml of aqueous solution. It was vigorously stirred and heated to a steaming point. To synthesize about 20–30-nm diameter AgNPs, 10–15-mL solution of sodium citrate was quickly added while steaming the AgNP solution. The solution was heated for another 10–15 min, and the final solution was allowed to cool naturally to room temperature (shown in **Figure 1**).

2.1.2. Peptide-coated AgNPs

Peptide-anchored silver nanoparticles were prepared by mixing citrated-capped AgNP with 0.5-mM peptide concentration in aqueous solution. The solution was stirred for about 10 min, and the self-assembled process was made for 20 h to get a uniform coating.

2.1.3. Characterization of silver nanoparticles

UV-visible absorption spectra were recorded at room temperature from 300 to 800 nm range. Fluorescence emission spectra were collected using a Horiba Fluoromax-4 spectrofluorometer. The chemical compositions of AgNPs solution were collected using a Fourier transform infrared spectroscopy ranging from 4000 to 400 cm^{-1}. The silver nanoparticles size and morphology of particles were determined by TEM using a Tecnai G2 F20. Samples were prepared by evaporating a 10-μL solution of AgNPs onto carbon-supported copper grids. For the determination of particle size, 300 particles were counted from multiple pictures from different areas of the TEM grid using Image J software analysis. The zeta potential of the particles was

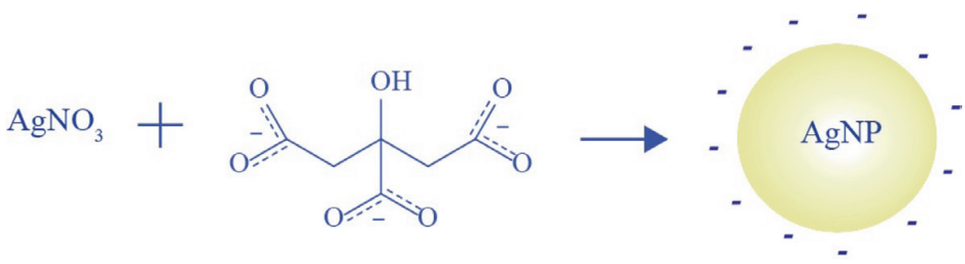

Figure 1. Schematic of silver nanoparticles (AgNPs) synthesis.

analyzed by using the Zetasizer Nano-ZS device. The measurements were carried out at room temperature at 25°C in aqueous solution. The zeta potential was calculated from the electrophoretic mobility based on the Smoluchowski theory.

3. Results and discussion

The peptide-capped-AgNPs size was analyzed by transmission electron microscopy (TEM) (**Figure 2**). The diameter and size distribution of the AgNPs were measured using TEM image analysis software and verified by image J software. The diameter of the silver nanoparticles was approximately observed to be 27 ± 2.0 nm (**Figure 2**), and it was measured by statistical analysis. The images of nanoparticles are shown in **Figure 2(a)–(c)** and peptide-anchored AgNPs images are also shown in **Figure 3(a)** and **(b)**. The peptide anchoring does not influence the size of silver nanoparticles. On the basis of the HR-TEM images, and the constant silver core diameter, it is evident that peptide-anchored-AgNPs remain mono-disperse even after peptide-anchoring process (**Figure 3**).

The HR-TEM image (**Figures 2** and **3**) of AgNPs showed that the fringe spacing of AgNP was 2.4 Å, which corresponded to the spacing between the plane of face-centered cubic (fcc) silver. The selected area of the diffraction pattern (SEAD) of silver nanoprism (**Figure 2(d)**) indicated that the entire nanoparticle was a single crystalline structure [32–34]. The SEAD pattern was

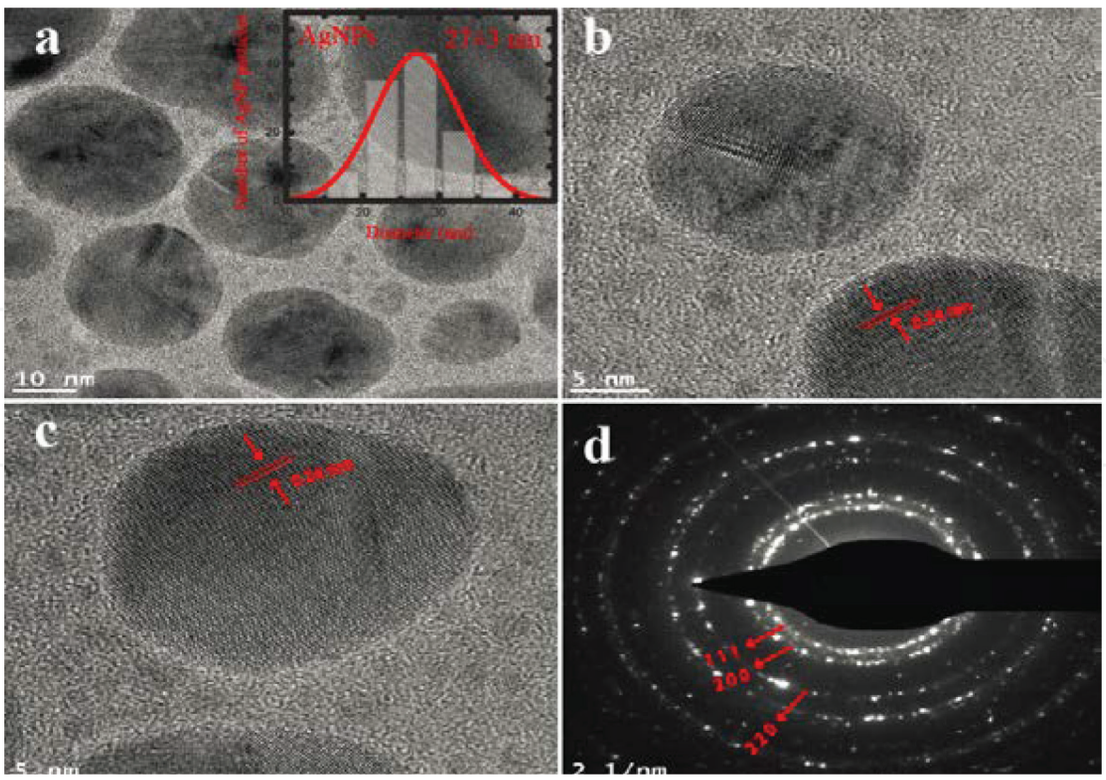

Figure 2. The TEM images of silver nanoparticles dispersion (a–c) and a selected area of the diffraction pattern of gold nanoparticles (d), and the insert shows the diameter distribution of AgNPs (a).

http://dx.doi.org/10.5772/intechopen.76829

indexed according to planes of (111) and (200) reflection, and the crystal structure of silver is FCC on the basis of the d-spacing 2.4 and 2.04 Å. The d-spacing was also calculated from diffraction pattern. The HR-TEM image of peptide-anchored AgNPs showed (**Figure 3**) that the nano-thin layer of peptide anchoring was observed.

The FTIR spectra of citrate-stabilized AgNPs were performed to know the anchoring molecules present on the surface of AgNPs (**Figure 4**). FTIR spectrum shows absorption bands at 3350, 2914, 2855, 2354, 1740, 1632, 1455, 1377, 1242, and 1040 cm^{-1} and indicating the presence of anchoring agent on the AgNPs surface. The bands at 3350 cm^{-1} in the spectra indicate an O–H stretching vibration in the presence of alcohol. The bands at 2914 and 2855 cm^{-1} regions arising from C–H stretching of the aromatic groups were found. The band at 1740 cm^{-1} was assigned to the C–C band stretching. The band at 1632 cm^{-1} in the spectra indicates C–C and C–N stretching in the presence of proteins [35]. The band at 1455 cm^{-1} was indicated for N–H stretch vibration in the presence of amide linkages of peptides. These functional groups have

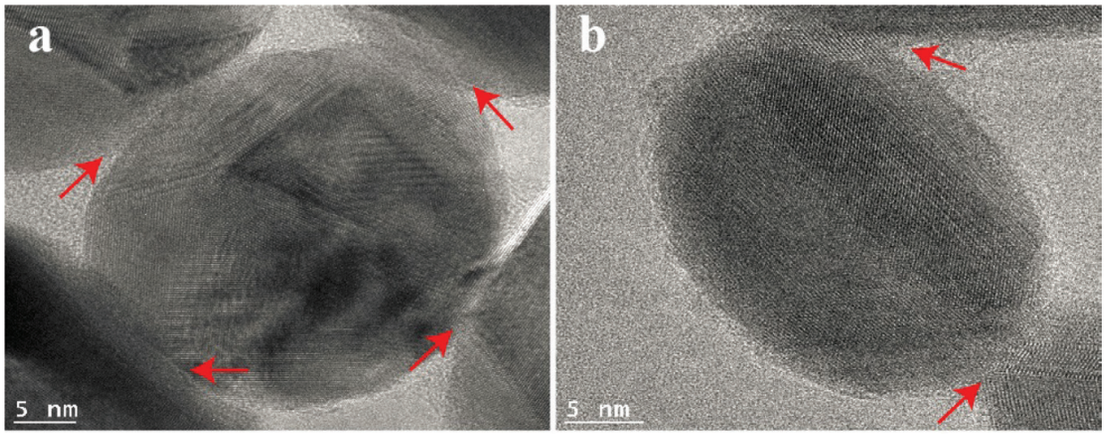

Figure 3. HR-TEM image of peptide-coated AgNPs.

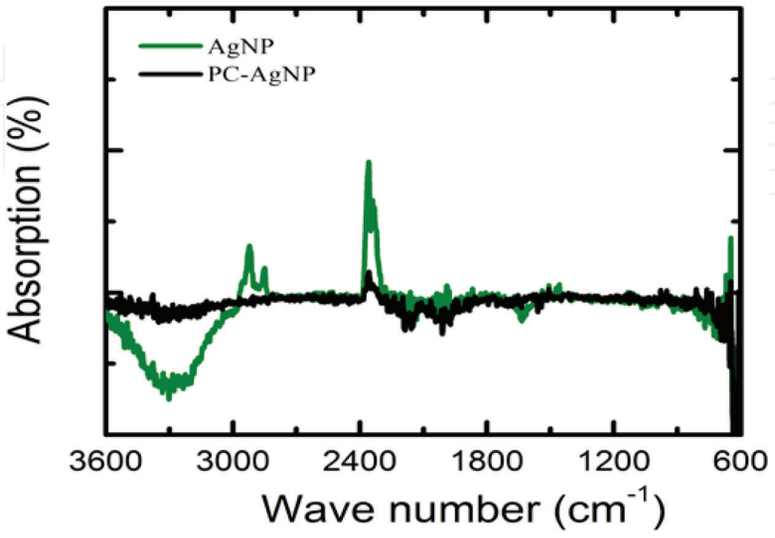

Figure 4. FTIR spectra of silver nanoparticles.

an important role in stability and anchoring of AgNP as reported in the previous studies [35]. The bands at 1455 and 1040 cm^{-1} were assigned for N–H and C–N stretch vibration of the proteins, respectively. The peptide-anchored AgNP particles spectra were also collected by using FTIR and observed that the peaks were suppressed. It may be due to a thin nano-layer anchoring covered on the nanoparticles surface.

The citrated-AgNPs show a Plasmon band at 529 nm (**Figure 5(a)**) with the help of UV-visible spectra. The particle diameter and size can also be identified from the concentration of silver nanoparticles solution [36–38]. The surface Plasmon absorption spectrum of AgNPs as the function of concentration is shown in **Figure 5(a)**. The intensity of absorption spectra increases as increasing the AgNP concentration. The trend was consistent with the changes indicating the surface of Plasmon band of AgNPs. For peptide (ID_3)-anchored AgNPs, the Plasmon band absorbance shifts to a higher wavelength of 404-nm region (**Figure 5(b)**).

The hydrodynamic diameter of peptide-anchored-AgNPs was measured by Zetasizer as 27 ± 2 nm. Zeta potential measurements indicate that the charge of the Cit-AgNP is −40 ± 2 mV (**Figure 6**) in a water medium and the charge of peptide-anchored-AgNPs is −13 ± 1 mV. The differences of charge are observed between citrated-AgNPs and PC-AgNPs in UV-visible region, and TEM and zeta potential measurements show evidence that the peptide is effectively anchored on the surface of AgNPs. The shift to a higher Plasmon band and the hydrodynamic diameter size increase by about 1–2 nm after the addition of a peptide which is consistent with the formation of a peptide layer on the surface of nanoparticles [18]. Also, the reduction of charge from −40 to −13 mV (**Figure 6**) indicates the displacement of negatively charged citric acid by the positive charge of the peptide. The small amount of negative charge still remaining on the PC-AgNPs is most likely due to a few residual citrate molecules on the surface even after ligand exchange.

The stability of peptide-anchored nanoparticles in phosphate-buffered saline is the first phenomenon for developing robust, biocompatible systems. However, if the particles are to be utilized in more complex environments, such as in vivo, then harsher conditions need to be analyzed.

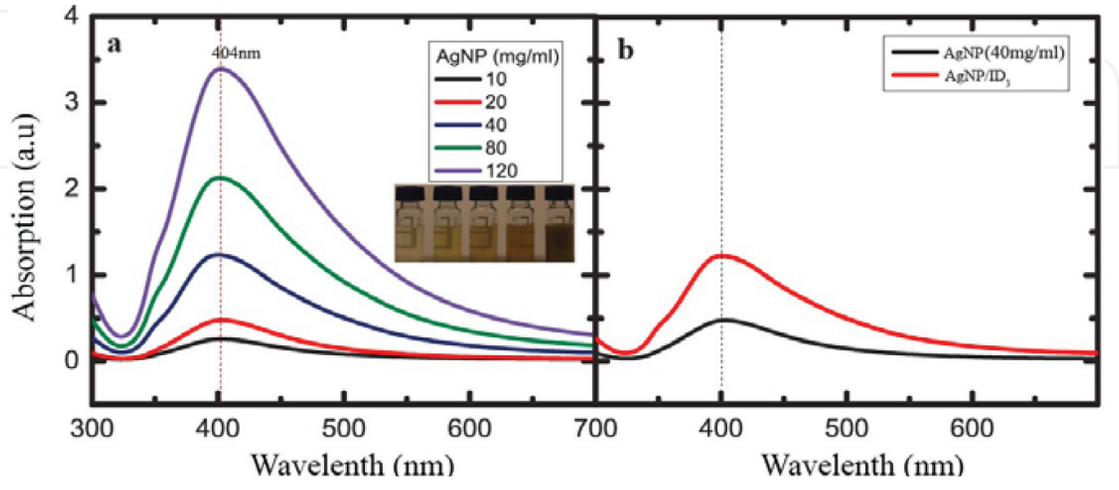

Figure 5. (a) Absorption spectra with a peak intensity of AgNPs at different concentrations. (b) Absorption spectra of AgNPs and $AgNP/ID_3$ at 30 mg/ml AgNP concentration.

Particle stability was assessed by monitoring the hydrodynamic diameter of nanoparticles using the UV–visible, TEM, and DLS. As seen in **Figure 7**, PC-AgNPs maintain the same hydrodynamic diameter (27 ± 2) after exposure to 15 wt% NaCl, 1 mg/ml lysozyme, and PBS solutions.

We examined the peptide-anchored AgNP stability under high salt conditions. Most of the nanoparticles aggregate when the salt was increased due to the screening of electrostatic repulsion. However, zwitterionic and mixed charge materials can resist aggregation of

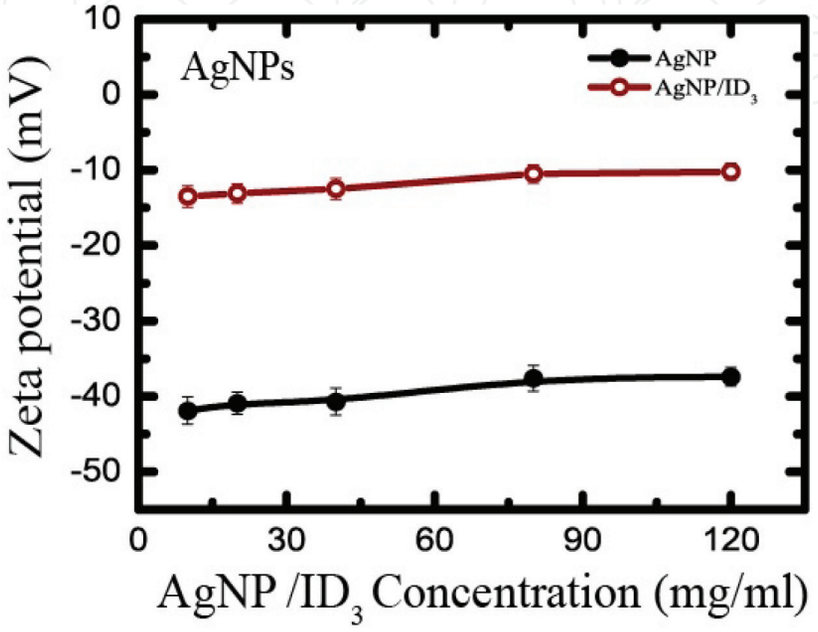

Figure 6. (a) The zeta potential of AgNPs and AgNP/ID_3 as a function of concentration.

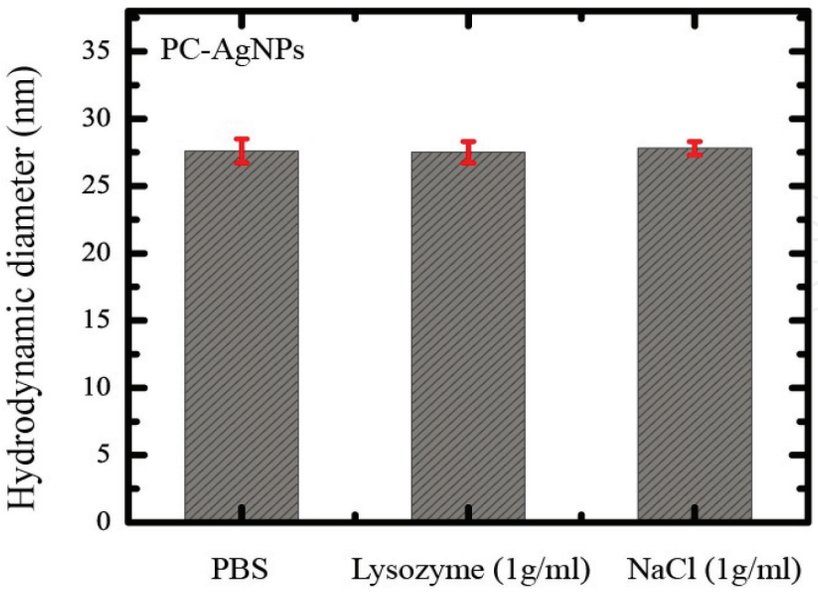

Figure 7. DLS measurements of the hydrodynamic diameter (volume percentage) (nm) of PC-AgNPs after exposure to PBS, 1 mg/mL lysozyme in PBS, and 15 wt% NaCl solution for 50 min. Each data point represents an average value/standard deviation from three independent measurements.

nanoparticles due to the presence of a strongly bound surface hydration layer [17, 18]. In addition, to examining particle stability in PBS medium, the stability of peptide-anchored AgNPs was also measured at higher salt concentrations. Peptide-anchored silver nanoparticles maintain stability even at 15 (wt%) salt concentration. These results indicate that the thin nano-peptide layer formed on the surface of silver nanoparticles (AgNPs).

4. Conclusion

In summary of results, the synthesis and characterization of peptide-anchored silver nanoparticles was demonstrated. The peptide-anchored nanomaterials were generated through a simple reduction approach, which helps a general synthetic route that produces particles of a similar size using peptides anchoring. The AgNPs were generally spherical with a relatively narrow size distribution. Peptide-anchored AgNPs show high stability in a high salt concentration. The results suggest that the reactivity of the peptide on AgNPs surface is governed by more details as indicated by the peptide structure. These results would be useful in the development of functional nanoparticles that exploit surface-based activity in the area of drug delivery and various bionanotechnology applications.

Acknowledgements

The authors would like to thank WPI, USA, and IISc, Bangalore, India, for the financial support.

Author details

Parvathalu Kalakonda[1]* and Sreenivas Banne[2]

*Address all correspondence to: parvathalu.k@gmail.com

1 Department of Chemistry, Chongqing University, Chongqing, People's Republic of China

2 Department of Materials Science and Engineering, Carnegie Mellon University, Pittsburgh, Pennsylvania, USA

References

[1] Baptista P, Pereira E, Eaton P, Doria G, Miranda A, Gomes I, Quaresma P, Franco R. Gold nanoparticles for the development of clinical diagnosis methods. Analytical and Bioanalytical Chemistry. 2008;**391**(3):943-950

[2] Dykman LA, Khlebtsov NG. Gold nanoparticles in biology and medicine: Recent advances and prospects. Acta Naturae. 2011;**3**(2):34-55

[3] Yeh YC, Creran B, Rotello VM. Gold nanoparticles: Preparation, properties, and applications in bionanotechnology. Nanoscale. 2012;**4**(6):1871-1880

[4] Han M, Gao X, Su JZ, Nie S. Quantum-dot-tagged microbeads for multiplexed optical coding of biomolecules. Nature Biotechnology. 2001;**19**(7):631-635

[5] Huang X, El-Sayed IH, Qian W, El-Sayed MA. Cancer cell imaging and photothermal therapy in the near-infrared region by using gold nanorods. Journal of the American Chemical Society. 2006;**128**(6):2115-2120

[6] Mirkin CA, Letsinger RL, Mucic RC, Storhoff JJ. A DNA-based method for rationally assembling nanoparticles into macroscopic materials. Nature. 1996;**382**(6592):607-609

[7] Moreno-Manas M, Pleixats R. Formation of carbon−carbon bonds under catalysis by transition-metal nanoparticles. Accounts of Chemical Research. 2003;**36**(8):638-643

[8] Salem AK, Searson PC, Leong KW. Multifunctional nanorods for gene delivery. Nature Materials. 2003;**2**(10):668-671

[9] Peng ZA, Peng X. Nearly monodisperse and shape-controlled CdSe nanocrystals via alternative Routes: Nucleation and growth. Journal of the American Chemical Society. 2002;**124**(13):3343-3353

[10] Puntes VF, Krishnan KM, Alivisatos AP. Colloidal nanocrystal shape and size control: The case of cobalt. Science. 2001;**291**(5511):2115-2117

[11] Choi CHJ, Zuckerman JE, Webster P, Davis ME. Transcytosis and brain uptake of transferrin-containing nanoparticles by tuning avidity to transferrin receptor. In: Proceedings of the National Academy of Sciences of the United States of America. 2011;**108**(16):6656-6661

[12] Albanese A, Chan WC. Effect of gold nanoparticle aggregation on cell uptake and toxicity. ACS Nano. 2011;**5**(7):5478-5489

[13] Karmali PP, Simberg D. Interactions of nanoparticles with plasma proteins: Implication on clearance and toxicity of drug delivery systems. Expert Opinion on Drug Delivery. 2011;**8**(3):343-357

[14] Larson TA, Joshi PR, Sokolov K. Preventing protein adsorption and macrophage uptake of gold nanoparticles via a hydrophobic shield. ACS Nano. 2012;**6**(10):9182-9190

[15] Kodiyan A, Silva EA, Kim J, Aizenberg M, Mooney DJ. Rigidity of two-component hydrogels prepared from alginate and poly(ethylene glycol)−diamines. ACS Nano. 2012;**6**(6):4796-4805

[16] Liu XS, Chen YJ, Li H, Huang N, Jin Q, Ren KF, Ji J. Tumor-Targeting and microenvironment-responsive smart nanoparticles for combination therapy of antiangiogenesis and apoptosis. ACS Nano. 2013;**7**(7):6244-6257

[17] Yang W, Zhang L, Wang SL, White AD, Jiang SY. Functionalizable and ultra stable nanoparticles coated with zwitterionic poly(carboxybetaine) in undiluted blood serum. Biomaterials. 2009;**30**(29):5617-5621

[18] Zhang L, Xue H, Gao CL, Carr L, Wang JN, Chu BC, Jiang SY. Maging and cell targeting characteristics of magnetic nanoparticles modified by a functionalizable zwitterionic polymer with adhesive 3,4-dihydroxyphenyl-l-alanine linkages. Biomaterials. 2010;**31**(25):6582-6588

[19] Collier JH, Segura T. Designing ECM-mimetic materials using protein engineering. Biomaterials. 2011;**32**(18):4198-4204

[20] Yoganathan V. Evaluation of the effects of antimicrobial peptides on endodontic pathogens In Vitro. Otago: Otago; 2012. p. 131

[21] Ansari MA, Khan HM, Khan AA. Anti-biofilm efficacy of silver nanoparticles against MRSA and MRSE isolated from wounds in a tertiary care hospital. Biologie et Médecine. 2011;**3**(2):141-146

[22] Naqvi SZ, Kiran U, Ali MI, Jamal A, Hameed A, Ahmed S, et al. Combined efficacy of biologically synthesized silver nanoparticles and different antibiotics against multidrug-resistant bacteria. International Journal of Nanomedicine. 2013;**8**:3187-3195. DOI: 10.2147/IJN.S49284. [PubMed: 23986635]

[23] Kora AJ, Arunachalam J. Bactericidal potential of silver nanoparticles synthesized using cell-free extract of *comamonas acidovorans*: In vitro and in silico approaches. World Journal of Microbiology and Biotechnology. 2011;**27**(5):1209-1216. DOI: 10.1007/s11274-010-0569-2

[24] Alizadeh H, Salouti M, Shapouri R. Actericidal effect of silver nanoparticles on intramacrophage brucella abortus. Jundishapur Journal of Microbiology. 2014;**7**(3):e9039

[25] Levy R, Thanh NTK, Doty RC, Hussain I, Nichols RJ, Schiffrin DJ, Brust M, Fernig DG. Ational and combinatorial design of peptide capping ligands for gold nanoparticles. Journal of the American Chemical Society. 2004;**126**(32):10076-10084

[26] Olmedo I, Araya E, Sanz F, Medina E, Arbiol J, Toledo P, Alvarez-Lueje A, Giralt E, Kogan MJ. Bioconjugate Chemistry. 2008;**19**(6):1154-1163

[27] Arosio D, Manzoni L, Araldi EM, Scolastico C. Cyclic RGD functionalized gold nanoparticles for tumor targeting. Bioconjugate Chemistry. 2011;**22**(4):664-672

[28] Kim YH, Jeon J, Hong SH, Rhim WK, Lee YS, Youn H, Chung JK, Lee MC, Lee DS, Kang KW, Nam JM. Tumor targeting and imaging using cyclic RGD-PEGylated gold nanoparticle probes with directly conjugated iodine-125. Small. 2011;**7**(14):2052-2060

[29] Scari G, Porta F, Fascio U, Avvakumova S, Dal Santo V, De Simone M, Saviano M, Leone M, Del Gatto A, Pedone C, Zaccaro L. Multidentate peptide for stabilization and facile bioconjugation of gold nanoparticles. Bioconjugate Chemistry. 2012;**23**(3):340-349

[30] Sun L, Liu D, Wang Z. Functional gold nanoparticle-peptide complexes as cell-targeting agents. Langmuir. 2008;**24**(18):10293-10297

[31] Reithofer MR, Lakshmanan A, Ping AT, Chin JM, Hauser CA. In situ synthesis of size-controlled, stable silver nanoparticles within ultrashort peptide hydrogels and their antibacterial properties. Biomaterials. 2014;**35**(26):7535-7542

[32] Chen S, Cao Z, Jiang S. Ultra-low fouling peptide surfaces derived from natural amino acids. Biomaterials. 2009;**30**(29):5892-5896

[33] Khan MAM, Kumar S, Ahamed M, Alrokayan SA, AlSalhi MS. Structural and thermal studies of silver nanoparticles and electrical transport study of their thin films. Nanoscale Research Letters. 2011;**6**(1):434

[34] Lin K, Yi J, Hu S, Sun J, Zheng J, Wang X, Ren B. Intraband Hot-Electron photoluminescence from single silver nanorods. ACS Photonics. 2016;**3**(7):1248-1255

[35] Prakash P, Gnanaprakasam P, Emmanuel R, Arokiyaraj S, Saravanan M. Green synthesis of silver nanoparticles from leaf extract of Mimusops elengi, Linn. for enhanced antibacterial activity against multi drug resistant clinical isolates. Colloids and Surfaces B: Biointerfaces. 2013;**108**:255-259

[36] Mogensen KB, Katrin K. Quantum size effects in the optical properties of ligand stabilized aluminum nanoclusters. The Journal of Physical Chemistry C. 2014;**118**(48): 28075-28083

[37] Kalakonda P, Banne S. Synthesis and optical properties of highly stabilized peptide-coated gold nanoparticles. Plasmonics. August 2017;**12**(4):1221-1225

[38] Kalakonda P, Banne S. Synthesis and optical properties of highly stabilized peptide-coated silver nanoparticles. Plasmonics. 2017;**12**(4):121-122. https://doi.org/10.1007/s11468-017-0628-8

IntechOpen